Autonomous Elevator Inspection with Unmanned Aerial Vehicle

Tsun Kit Hui and Huiying Chen, *The Hong Kong Polytechnic University*

Abstract— Hong Kong has the highest elevator density in the world, with more than 63,000 elevators. The inspection and maintenance of elevator rope have been carried out directly by human with simple inspection gadgets traditionally. Recently however, the big gap between dramatically increasing demand of elevator inspection and insufficient manpower in the related industry, as well as the safety issues coupled with human inspection have resulted in investigations of the possibility in adopting Unmanned Aerial Vehicle (UAV) for elevator rope inspection. Nevertheless, UAV's control and navigation in a relatively small (comparing to the size of UAV itself) elevator shaft with extremely low luminance and high air turbulence are the biggest challenges in this solution, especially when its bottom camera, which serves as a crucial input for hovering, is nearly unplugged. This project intends to propose and develop an effective methodology of elevator rope inspection with an UAV. Vision-based control and navigation algorithms for facilitating the UAV with autonomous elevator rope detection, tracking, and inspection have been proposed. Simulations and experiments were conducted with a real setup of elevator shaft. Experimental results verified the effectiveness and efficiency of the proposed method. The proposed method can address the above issues confronted by the elevator maintenance service providers.

Keywords—UAV, Computer Vision, SLAM, Indoor Navigation

I. INTRODUCTION

HONG Kong is a vertical city with the highest elevator density in the world, with more than 63,000 elevators in use, totaling 30 million trips each day. However, the rate of elevator accidents has been increasing dramatically in the last five years. According to Table 1, the number of reported accidents has risen from 248 in 2010 to 483 in 2015, 94.8 percent increase. Moreover, there are insufficient elevator technicians in Hong Kong to inspect and maintain the elevators.

Table 1 Number of elevators' accidents in Hong Kong [1]

Year	2010	2011	2012	2013	2014	2015
No. of accidents	248	257	283	330	446	483

A. Elevator Maintenance Accident

According to the Lifts and Escalators (Safety) Ordinance Chapter 327, elevator owners need to ensure that only registered contractors and engineers are engaged in repair and maintenances work. Elevators need to be cleaned, oiled, and inspected monthly. Their safety equipment also needs to be tested annually and other devices every five years. This frequent safety testing, however, overlooks the dangers, at times lethal, of working inside an elevator shaft. Specifically, according to the Elevators Unit in New York, 75% of serious accidents during elevator maintenance happened in the elevator shaft (*Fig.1*).

The majority of these accidents occur because of improper or inadequate fall protection. In fact, approximately half of those killed in elevator accidents are killed from falling down the shaft. About one-third of elevator fatalities are caused by workers caught between or struck by objects. A small number of fatalities are also caused by electrocution. Worker injury or death involving elevators can usually be traced to one of the following factors [2]:

- Electric shock or electrocution
- Being struck by the elevator or counterweight
- Getting caught in the door or other moving parts
- Falling from the elevator car
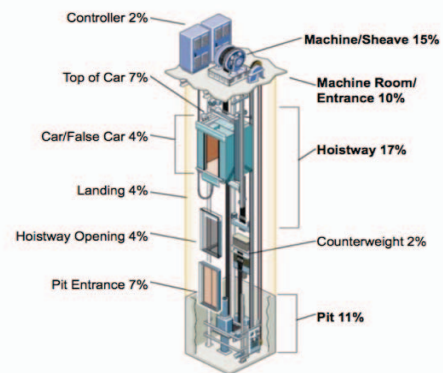- Asphyxiation while trapped in the elevator
- Falling into the elevator shaft

Fig.1 Probability distribution of accidents happened during elevator maintenance

B. Difficulties in Traditional Maintenance

Besides the serious safety issues, there are other difficulties in traditional maintenance methods: (a) lack of qualified technicians, (b) high cost, (c) lack of standardization in the elevator maintenance service industry, and (d) unreachable zone induced inspection loopholes.

Finally, since traditional inspection is conducted manually, maintenance quality differs widely among the industry. In addition, part of the elevator rope is never exposed to the technicians during maintenance. For example, some buildings have dedicated elevators for high zone floors and low zone floors, elevator technicians do not have a proper way to check the elevator rope between high zone and low zone floors, these areas are the unreachable zone to the technicians. Hence, elevator maintenance service providers seek modern technologies to solve these difficulties.

C. New Exploration in Elevator Rope Inspection

The Electrical and Mechanical Services Department (EMSD) of Hong Kong Government and different elevators maintenance service providers like KONE Elevator(HK) Ltd. looked for different technologies and tried to use an UAV to solve the difficulties of traditional elevator inspection methods. However, they encountered five major obstacles when implementing their ideas. (a) The limited size of elevator shaft prohibits the navigation of the UAV. It is easy for the UAV to crash into walls, rope or other mechanical components in the elevator shaft. (b) It is hard to manually control the UAV in elevator shaft.

The human controller has to avoid crashing the UAV and inspect the rope at the same time. It is difficult for single individual to simultaneously execute both actions. Also, The UAV blocks most of the sight of the controller because of the narrow and long shape of the elevator shaft. Furthermore, parallax distorts human's depth perception, making it even more difficult for human controller to maneuver the UAV properly. (c) It is dark in the elevator shaft. Computer vision needs certain level of luminance to capture a clear image and then process the image information. (d) UAV has a limited flight time of around 25 minutes. The UAV needs to complete the whole inspection within the limited time frame. (e) There is a lack of well-developed algorithms for accurate inspection.

II. THE PROPOSED METHODOLOGY

In this project, I aimed to develop an autonomous elevator rope inspection system with UAVs. The objectives of the system are an Unmanned Aerial System (UAS) which solves the difficulties encountered by the industry. The specifications are as follows: to reduce human control of the UAVs as much as possible since elevator technicians are not trained to control UAVs; to have UAVs be able to autonomously fly along the elevator shaft and find the defects; and to have them be able to perform long inspection runs. The key issues that need to be solved here are position control, automatic rope tracking, communication, image acquisition and automatic fault detection.

Four modules need to be built in order to accomplish the objectives. They are the Image Process Module, the Simultaneous Localization and Mapping (SLAM) Module, the Navigation and Control Module and the Visual Inspection Module. The flowchart of these programs is displayed in *Fig.2*. First, the technicians input some basic data into the system through a graphical user interface, including: number of ropes, diameter of rope, height of the building, and size of the elevator shaft. Then, the system receives images from the UAV through Wireless LAN and analyzes them. Template Matching is used to locate the rope in the image and a Distance Regression Model is used to determine the distance between the rope and the UAV. The rope position is then saved in a SLAM which also saves all of the previous rope position data. If the rope is found on the image, the navigation module sends a signal to the UAV to navigate along the rope. If the rope is not found on the image, the system looks into the SLAM and calculates the highest possible coordinate at which the UAV can find the rope. The system loops 30 times per second.
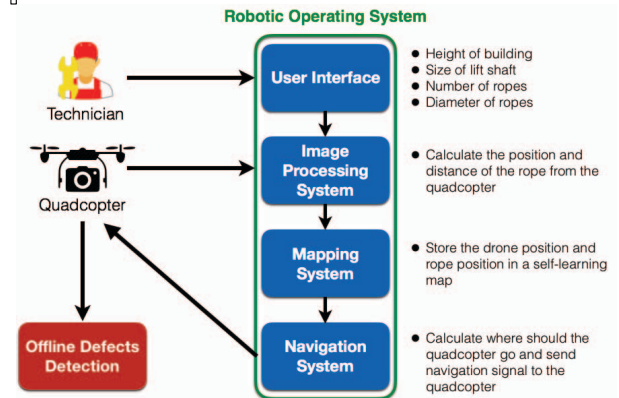

Fig.2 Basic flowchart of the Unmanned Aerial System for autonomous elevator rope inspection

Fig.3 Rouging and rusting of elevator rope

A. Elevator Rope Defect's Criteria

Ropes are classified by the number of strands as well as by the number of wires in each strand. There are three major defects in elevator rope which are rouging, rusting and under-sizing. Rouge is a fine, red iron oxide which forms on the rope, giving it a "rusty" appearance and suggesting that advanced deterioration is taking place (*Fig.3*). Rouging is caused by fretting, a special type of abrasion which occurs when two solid surfaces bear against one another, while under a heavy load and subjected to small amplitude vibrations. Rouge is different from what we commonly refer to as rust. Rust forms when moisture is introduced to a metal surface. When combined with this moisture, the metal surface, itself, rusts. Moreover, if the diameter of the elevator rope reduces by 10%, it is considered as defected. Normally, the elevator car is held by four to six elevator ropes. If any defect is found on any of the rope, the whole set of ropes need to be replaced.

B. Observation Model

The observation model takes an important role in the development of the UAS. It is important to find the connection between the UAV coordination system and the world coordination system. A universal coordination system is set up for a better communication within the UAS. Writing out all of the elements of the composite rotation,

$$R = \begin{bmatrix} \cos\alpha\cos\beta\cos\gamma - \sin\alpha\sin\gamma & -\cos\alpha\cos\beta\sin\gamma - \sin\alpha\cos\gamma & \cos\alpha\sin\beta \\ \sin\alpha\cos\beta\cos\gamma + \cos\alpha\sin\gamma & -\sin\alpha\cos\beta\sin\gamma + \cos\alpha\cos\gamma & \sin\alpha\sin\beta \\ -\sin\beta\cos\gamma & \sin\beta\sin\gamma & \cos\beta \end{bmatrix} \quad (1)$$

is the defined rotational matrix. To complete the observation model, translation is needed from camera coordinate to world coordinate by adding a column vector $[Tx \quad Ty \quad Tz]^T$, and for consistency both sides' number of row to perform matrix multiplication, it is augmented to be homogeneous coordinates, expressed as

$$\begin{bmatrix} X_w \\ Y_w \\ Z_w \\ 1 \end{bmatrix} = \begin{bmatrix} & & & Tx \\ & R_{3\times3} & & Ty \\ & & & Tz \\ 0 & 0 & 0 & 1 \end{bmatrix} \begin{bmatrix} X_c \\ Y_c \\ Z_c \\ 1 \end{bmatrix} \quad (2)$$

C. Rope Recognition Algorithm

The Rope Recognition Algorithm is built based on template matching and a tailor-made distance regression model. Below is a brief explanation of basic **SAD** (Sum of Absolute Differences) Template matching [3]. Template matching is used to find the rope position of the acquired image from the UAV and the distance regression model finds the distance between the rope and the UAV. Template matching can be easily performed on grey images. This technique is implemented by first picking out a part of the search image to use as a template: The search image is defined as $S(x,y)$, where (x, y) represents the coordinates of each pixel in the search image. $T(x_t,y_t)$ is the template image, where (x_t,y_t) represents the coordinates of each pixel in the template. The center (or the origin) of the template $T(x_t,y_t)$ simply moves over each (x,y) point in the search image and calculate the sum of products between the coefficients in $S(x,y)$ and $T(x_t,y_t)$ over the whole area spanned by the template. As all possible positions of the template with respect to the search image are considered, the position with the highest score is the best position. This method is sometimes referred to as 'Linear Spatial Filtering' and the template is called a filter mask.

For example, one way to handle translation problems on images, using template matching is to compare the intensities of the pixels, using the **SAD** measure. A pixel in the search image with coordinates (x_s,y_s) has intensity $I_s(x_s,y_s)$ and a pixel in the template with coordinates (x_t,y_t) has intensity $I_t(x_t,y_t)$. Thus the absolute difference in the pixel intensities is defined as **Diff$(x_s, y_s,x_t,y_t) = | I_s(x_s,y_s) - I_t(x_t,y_t) |$**.

$$SAD(x,y) = \sum_{i=o}^{T_{rows}} \sum_{j=o}^{T_{cols}} Diff(x+i, y+j, i, j) \quad (3)$$

is the mathematical representation of the idea about looping through the pixels in the search image as we translate the origin of the template at every pixel and take the SAD measure is the following:

$$\sum_{x=o}^{S_{rows}} \sum_{y=o}^{S_{cols}} SAD(x,y) \quad (4)$$

S_{rows} and S_{cols} denote the rows and the columns of the search image and T_{rows} and T_{cols} denote the rows and the columns of the template image, respectively. In this method the lowest SAD score gives the estimate for the best position of template within the search image. $R(x, y)$ is the map of comparison result. If search image is $W \times H$ and template image is $w \times h$, then result is $(W - w + 1) \times (H - h + 1)$. In order to increase the accuracy of the template matching, a template matching of normalized correlation coefficient is used [4][5]. The method is defined by

$$R(x, y) = \frac{\sum_{(x',y')}\left(T(x', y') \cdot I(x + x', y + y')\right)}{\sqrt{\sum_{(x',y')} T(x', y')^2 \cdot \sum_{x',y'} I(x + x', y + y')^2}} \quad (5)$$

which $T(x', y')$ is denoted by

$$T(x', y') - \frac{1}{w \cdot h} \cdot \sum_{(x'',y'')} T(x'', y'') \quad (6)$$

and $I'(x + x', y + y')$ is denoted by

$$I(x + x', y + y') - 1/(w \cdot h)) \cdot \sum_{(x'',y'')} I(x + x', y + y')^2 \quad (7)$$

The minimum point in $R(x, y)$ is found to be the best matching point in **S(x, y)**. The template image used in the program is shown in *Fig.4* which is a close shot of the elevator rope. The screwing pattern of the elevator rope is clearly shown and provides a good result in rope recognition. After finding the minimum point in $R(x, y)$, a white square is cropped on the source image to recognize the rope position on the image like *Fig.5*. In order to determine the rope position in the horizontal-axis, the source image is divided into four equivalent areas. Depends on which area do the top-left vertex and the bottom-right vertex of the white square located, rope location on the horizontal-axis can be calculated. Although more areas can be divided in the image for a more accurate position of the rope, this increase the computational burden. Moreover, using four areas are sufficient enough to calculate the position of the rope since seven different results will be generated.

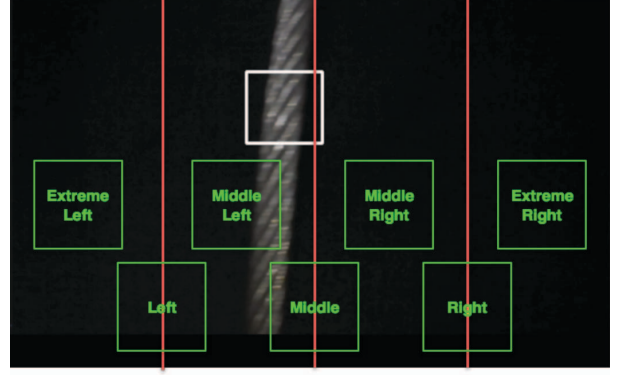**Fig. 4** Template image used in the program

Fig. 5 Template recognition of the rope(white box) and seven possible results of the rope position(green box)

However, there are errors induced by applying template matching as recognition algorithm for elevator rope inspection. Since template matching search for the minimum point in $R(x, y)$, even if the rope is not shown in the image, the algorithm will still generate a result and crop an irrelevant object in the image. This affected the accuracy of the rope tracking algorithm. Moreover, due to the low luminance level inside the elevator shaft, the camera often received black image. A tailor-made algorithm and approach were developed to solve the two problems and find the distance from the UAV to the elevator rope. This approach is only applicable in low luminance space. By adding an external torch to the UAV, it is possible to recognize, track and inspect the elevator rope.

The system will first turn the image into binary image by preset threshold. Here, the matter is straight forward. A comparison of each pixel intensity value with respect to a threshold is performed. If pixel value is greater than a threshold value, it is assigned as 1 (white pixel), otherwise it is assigned as 0 (black pixel). It separates out regions of an image corresponding to objects which we want to analyze. This separation is based on the variation of intensity between the object pixels and the background pixels. It helps to differentiate the pixels we are interested in from the rest (which will eventually be rejected). The threshold operation can be expressed as

$$dst(x, y) = \begin{cases} maxVal & if\ src(x, y) > thresh \\ 0 & otherwise \end{cases} \quad (8)$$

In order to solve the issue mentioned in the rope recognition algorithm section, a threshold was set for running the template matching. For instance, the template matching runs when the number of white

pixels is in between of 0 to 90000. This avoided the mismatch of the template matching algorithm when it receives a black image or the drone is too close to any object like wall. In this case, the accuracy of the elevator rope recognition increased dramatically. Moreover, the relationship of distance and number of white pixels was studied. When the elevator rope is closer to the drone camera, the number of white pixels is larger, vice versa. After extracting more than 2000 data to find the relationship of the distance and number of white pixels, a graph was plotted as *Fig.6*. Afterward, different mathematic models were used to find the best regression model to relate distance and the number of white pixels. The best regression model is logarithmic regression as shown in *Fig.6*.
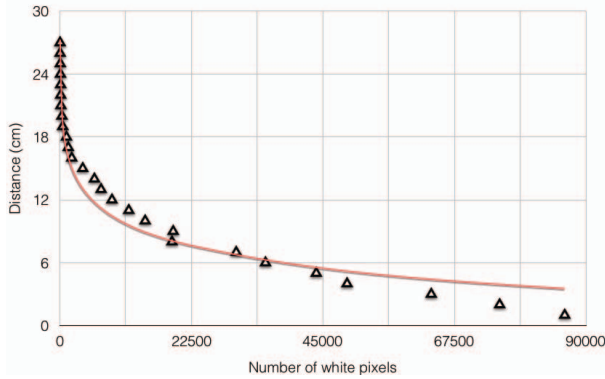

Fig.6 Logarithmic Regression of Distance(cm) versus number of white pixels

With the high coefficient of determination of 0.9758, this regression model is accurate in calculating the distance between the elevator rope and the UAV from the number of white pixels. This finding introduce a new way to find object distance and build SLAM in low luminance environment. With the low computational burden of this algorithm, it is useful in real time applications. The equation used to calculate the distance is

$$y = -3.0857 \, ln(x) + 38.591. \qquad (8)$$

where y is the distance between elevator rope and camera and x is the number of white pixels on the image. After getting the position and the distance of the elevator rope, this information was passed to the rope tracking algorithm.

D. Rope Tracking Algorithm

The Rope Tracking Algorithm enables the UAV to track the elevator rope automatically. There are two parts in the rope tracking algorithm. The first part is the SLAM for storing the rope information and generating a real time map [6]. The second part is a navigation and control system to send navigation commands to the UAV. Most the the SLAM developed are only applicable in light environment. Low luminance space like elevator shaft provide much less visual information then normal condition, making the well-developed SLAM not apply in this project. Therefore, I developed a new SLAM system to calculate the coordination of the drone and the coordination of the elevator rope. By integrating both IMU and camera images, a simple SLAM is built. Two 11 x 11 matrices are created to store the UAV location and rope location separately. matrix D_{11x11} stores the UAV location. By assuming the camera as the center of the UAV, data of IMU was used to estimate the UAV location. The *1* in the matrix represents the UAV location and each entry in Matrix D represents 5cm. Matrix D is a single-entry matrix where

$$D = \begin{bmatrix} 0 & \cdots & 0 \\ \vdots & 1_{5,5} & \vdots \\ 0 & \cdots & 0 \end{bmatrix}_{11x11} \qquad (9)$$

Fig.7 represents an example that the UAV moves to the right from time t to time $t+1$. Since D is a single-entry matrix, the only entry 1 represent the location of the UAV. The entry changed from $D_{6,6}$ to $D_{8,6}$ to represent the movement of the UAV.

Fig.7 *Change of Matrix D from time t to time t+1*

Matrix R is a zero matrix during initialization where all of the the past rope positions are stored here. Matrix R looks like

$$R = \begin{bmatrix} 0 & \cdots & 0 \\ \vdots & \ddots & \vdots \\ 0 & \cdots & 0 \end{bmatrix}_{11x11} \qquad (10)$$

Since the rope location is calculated from the position of UAV, R is a reference coordination system relies on Matrix D. Therefore, even if the

UAV loses the rope, the system enables the UAV to find the elevator rope in the narrow elevator shaft from its past data.

E. Rope Inspection Algorithm

After executing the previous algorithm successfully, a video is stored for inspection. There are two kinds of inspection needed: the rusting and rouging detection and the under sizing detection. Both of these are important for the safety of the elevator. When any red rust or rouge is spotted along the rope, the whole set of ropes needs to be replaced. Therefore, the target of this algorithm is to detect the red rouge and rust. The algorithm first turns the image into a Hue, Saturation, and Value (HSV) image, then searches for the color code of rust and rouge. Traditionally, RGB image layer is used for image extraction; the disadvantage, however, is the large influence of the lighting source. Considering the low luminance level in elevator shaft, HSV method is applied to extract the rusting and rouging region. The conversion work of HSL is given by [7]

$$H = \begin{cases} 60° \times \left(\frac{G'-B'}{\Delta} mod 6\right), C_{max} = R' \\ 60° \times \left(\frac{B'-R'}{\Delta} + 2\right) \ , C_{max} = G' \\ 60° \times \left(\frac{R'-G'}{\Delta} + 4\right) \ , C_{max} = B' \end{cases} \quad (11)$$

$$S = \begin{cases} 0 \quad , C_{max} = R' \\ \frac{\Delta}{C_{max}}, C_{max} \neq 0 \end{cases} \quad (12)$$

$$V = C_{max}. \quad (13)$$

After converting the image from RGB into HSV. The program stores the color range of rusting and rouging in HSV. Therefore, the algorithm could detect any pixel with values indicating rusting or rouging. The under-sizing detection algorithm involves five processes to generate accurate results. The ultimate goal of this algorithm is to detect the edge of the rope and find the distance between the two parallel edges. Then it calculates the width of the elevator rope using trigonometry, by measuring the distance from the UAV to the rope. The calculated width should be the same as diameter of the rope. Afterward, the calculated diameter, with the technicians' input, are compared to the rope's original diameter. If the diameter of the rope is reduced by more than 10%, the rope has to be replaced. The algorithm first turns the image from RGB into grayscale. Then, an adaptive threshold is applied to preserve more information on the image. Afterwards, a series of morphology operations filter out irrelevant. Next, the Zhang-Suen thinning algorithm [8] is applied to reduce the edge of the rope

into one pixel. Finally, a Hough Transform [9] is used to find the two edges of the elevator rope. The distance between the two edges is calculated by counting the number of pixels.
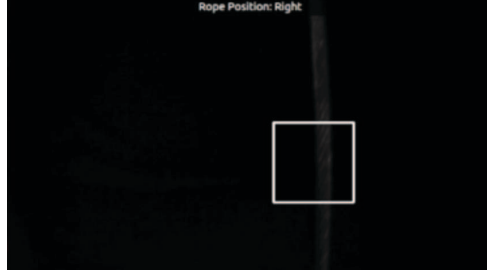
III. EXPERIMENT AND RESULTS

Experiments were conducted in order to test the accuracy and efficacy of the proposed methodology, a commercial UAV with the algorithm installed was tested in a simulated elevator shaft. As for platform, the Parrot AR.Drone, a commercially available quadcopter, was used. Compared to other modern UAV's such as Ascending Technology's Pelican or Hummingbird quadcopters, The Parrot has a very low price, quite robust and can, safely, be used indoor and close to people. This however comes at the price of flexibility: Neither the hardware itself nor the software running onboard can easily be modified, and communication with the quadcopters is only possible over wireless LAN. With battery and hull, the AR.Drone measures 53 cm × 52 cm and weights 420 g.

The AR.Drone is equipped with a 3-axis gyroscope and accelerometer, an ultrasound altimeter and two cameras. The first camera is aimed forward, covers a field of view of 73.5∘ × 58.5∘, has a resolution of 320 × 240 and a rolling shutter with a delay of 40 ms between the first and the last line captured. The video of the first camera is streamed to a laptop at 18 fps, using lossy compression. The quadcopter sends gyroscope measurements and the estimated horizontal velocity at 200Hz, the ultrasound measurements at 25Hz to the laptop. The raw accelerometer data cannot be accessed directly. The onboard software uses these sensors to control the roll Φ and pitch Θ, the yaw rotational speed $\dot{\Psi}$ and the vertical velocity $\dot{z}$ of the quadcopter according to an external reference value. This reference is set by sending a new control command u = $(\Phi, \Theta, \dot{z}, \Psi) \in [-1, 1]$ every 10 ms.
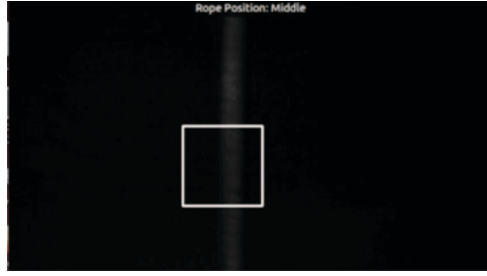
The Rope Recognition Algorithm provides an accurate result of both position measurement and distance measurement. For position measurement, the measurement result is 100% correct even the image is blurred. *Fig.8* shows the result of the position measurement algorithm, the template matching algorithm is capable to recognize the elevator rope even in a extremely dark environment, moreover, the algorithm categorizes the rope into several groups of direction like extreme left, left, middle, etc and send these information to the SLAM.
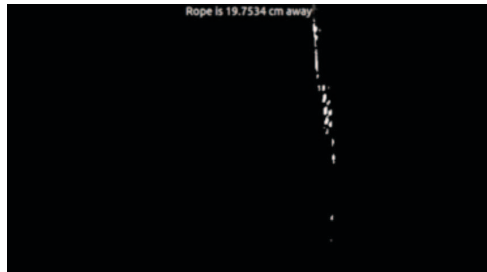
(a) Position detected: left

(b) Position detected: right

(c) Position detected: middle

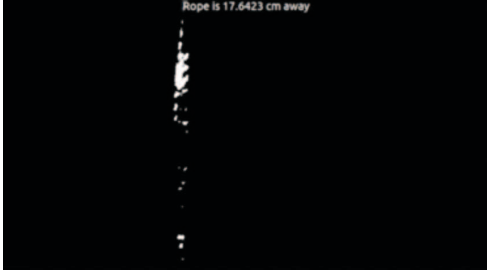*Fig.8* Result of rope position measurement

For the distance measurement, the accuracy is similar to the coefficient of determination (0.9758) which is 0.9705. This algorithm uses simple mathematic to estimate the rope co-ordination towards the UAV. Result of the algorithm is shown in *Fig.9*. It is surprising that the reflected luminance from the object can be used to calculate distance accurately in extremely dark environment. However, the luminance level of the torch has to be calibrated before use.
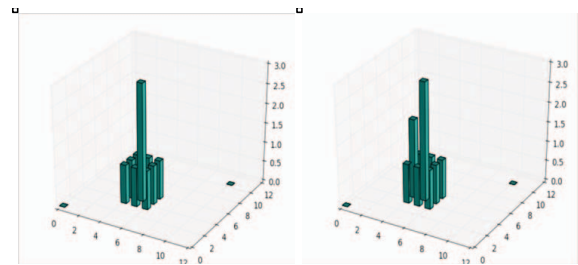

(a) Distance detected: 19.7534 cm

(b) Distance detected: 24.6718 cm

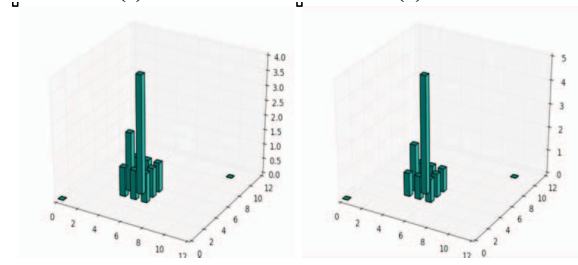(c) Distance detected: 17.6423 cm

Fig.9 Result of rope distance measurement

The low computational power enables real time application. The SLAM plot starts when t = 0 and updates the plot per second (*Fig.10)*. One unit in the z-axis represents 100 record of rope location. It means that when one hundred more rope locations are recorded at the same coordination, the bar at that coordinate will increase by 1 unit. The higher the bar the higher the chance the elevator rope is located at that spot. From the 50 tests on verifying the accuracy of SLAM, the highest bar coordination is always equal to elevator rope actual coordination. This is a reliable algorithm to find the elevator rope when the UAV loses the rope in its image.

(a) t=1

(b) t=2

(c) t=3

(d) t=4

Fig.10 Result of Simultaneous Localization and Mapping Algorithm

Although the result of Hough Transform seems convincing, the measure of the width is not accurate. There are too many steps involved to extract the two lines and each step has its own error. Especially at the stage of dilation and Zhang Suen Thinning Algorithm, both operations can only preserve 90% of the image information on elevator rope. The accuracy of the under-sizing algorithm was strongly affected by these two operations. The overall accuracy of the under-sizing detection algorithm is 73.12%. Since the elevator rope is considered defect when its diameter reduces by more than 10%, the algorithm is not precise enough to measure the diameter of the rope. However, the result from the algorithm can be a good reference for the elevator technicians since the elevator technicians only measure three samples of the whole rope during inspection. The system is able to enhance the quality of elevator inspection. Different image results of the under-sizing detection algorithm are shown in *Fig.11*.

(a) Source Image   **(b)** Grayscale Image

(c) Binary Image   **(d)** Dilated Image

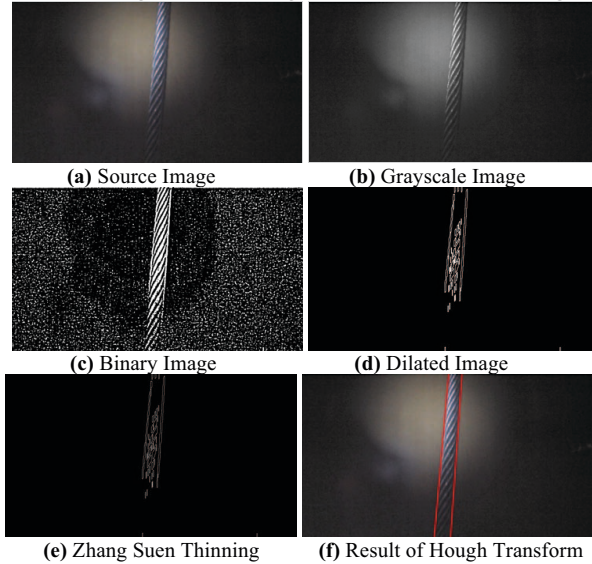**(e)** Zhang Suen Thinning   **(f)** Result of Hough Transform

Fig. 11 Simulation of under-sizing detection

The rouging and rusting detection shows a prefect result, Although the result is hard to quantify, all of the rouge and rust visible to the naked eye was detected by the algorithm. Moreover, the algorithm was able to detect rouge and rust that human eyes are not able to witness at a glance. This algorithm will be a great assist to the elevator technicians.
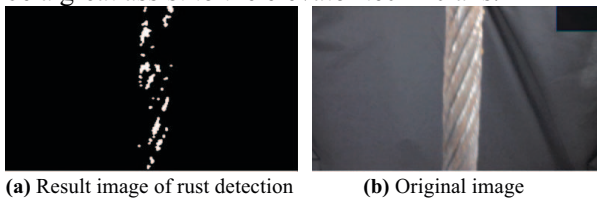

(a) Result image of rust detection   **(b)** Original image

Fig.12 Rusting and rouging extraction

IV. CONCLUSION

With the increasing elevator accident rate in Hong Kong, new technology is needed to improve the maintenance quality. However, various difficulties were faced by the related parties. An Unmanned Aerial System (UAS) was built to solve the safety issues and other difficulties came across in traditional elevator inspection. First, the UAS dramatically reduces the time elevator technicians spent in the dangerous elevator shaft. Second, it standardizes inspection criteria and performed a holistic inspection. Third, it easily accesses previously unreachable zones. Fourth, it reduces the cost of elevator maintenance and relieves the manpower of elevator technicians. Moreover, this has been backed by experimental results. The algorithm enables the UAV to inspect the elevator rope autonomously. New distance regression model and SLAM system are developed and show a good result of 97.58% accuracy when calculating distance with one camera. This project proves the feasibility of replacing human with UAV under jeopardous working situation like elevator shaft.

V. REFERENCES

[1] *Reported Lift Accident Records,* Electrical and Mechanical Services Department, Hong Kong Special Administrative Region, 2015.

[2] Comparison of worldwide lift safety standards, *"ISO Standard 11071,"* International Organization for Standardization, 2004.

[3] Sarvaiya, Jignesh N., Suprava Patnaik, and Salman Bombaywala. "Image registration by template matching using normalized cross-correlation."*Advances in Computing, Control, & Telecommunication Technologies*, 2009.

[4] A. Mahmood and S. Khan, "Correlation-Coefficient-Based Fast Template Matching Through Partial Elimination," in *IEEE Transactions on Image Processing*, vol. 21, no. 4, pp. 2099-2108, April 2012.

[5] Junzhi Guan *et al*., "PhD forum: Correlation coefficient based template matching for indoor people tracking," *Distributed Smart Cameras (ICDSC), 2012 Sixth International Conference on*, Hong Kong, 2012, pp. 1-2.

[6] B. P. W. Babu, D. Cyganski and J. Duckworth, "Gyroscope assisted scalable visual simultaneous localization and mapping," *Ubiquitous Positioning Indoor Navigation and Location Based Service, 2014*, Corpus Christ, TX, 2014, pp. 220-227.

[7] S. Supannarach and D. Thanapatay, "The study of using RGB color sensor to measure the Curcuminiods amount in Turmeric (Curcuma longa Linn.) and Zedoary (Curcuma Zedoarie Rose.) by comparing colors with HSL system,"*Electrical Engineering or Electronics Engineering, Computer, Telecommunications and Information Technology, 2008. ECTI-CON 2008. 5th International Conference on*, Krabi, 2008, pp. 529-532.

[8] W. Chen, L. Sui, Z. Xu and Y. Lang, "Improved Zhang-Suen thinning algorithm in binary line drawing applications," *Systems and Informatics (ICSAI), 2012 International Conference on*, Yantai, 2012, pp. 1947-1950.

[9] Dagao Duan, Meng Xie, Qian Mo, Zhongming Han and Yueliang Wan, "An improved Hough transform for line detection," *2010 International Conference on Computer Application and System Modeling (ICCASM 2010)*, Taiyuan, 2010, pp. V2-354-V2-357